Climate feedback implied by observed radiation and precipitation changes with midlatitude storm strength and frequency

George Tselioudis
Department of Applied Physics and Applied Mathematics, Columbia University, New York, New York, USA
NASA Goddard Institute for Space Studies, Columbia University, New York, New York, USA

William B. Rossow
NASA Goddard Institute for Space Studies, Columbia University, New York, New York, USA

Received 30 August 2005; revised 26 October 2005; accepted 7 December 2005; published 24 January 2006.

[1] Current climate observations are used to quantify the relationships between midlatitude storm strength and frequency and radiation and precipitation properties. Then, the derived radiation/precipitation-storm relationships along with the midlatitude storm changes with climate-warming predicted by a climate model are used to determine the radiation and precipitation changes resulting from an increase in midlatitude storm intensity and a decrease in midlatitude storm frequency. Increases in midlatitude storm intensity produce shortwave cooling and longwave warming while decreases in storm frequency produce the opposite effects. When the two changes are added together the increase in storm strength dominates producing a shortwave cooling effect of 0–3.5 W/m^2 and a longwave warming effect of 0.1–2.2 W/m^2. For precipitation, the increase in storm intensity also dominates the decrease in storm frequency and produces an increase in precipitation of 0.05–0.08 mm/day. **Citation:** Tselioudis, G., and W. B. Rossow (2006), Climate feedback implied by observed radiation and precipitation changes with midlatitude storm strength and frequency, *Geophys. Res. Lett.*, *33*, L02704, doi:10.1029/2005GL024513.

1. Introduction

[2] Clouds, radiation, and precipitation in midlatitudes are determined to a large extent by the frequency and amplitude of baroclinic waves. Several studies have examined cloud and radiation changes with dynamical parameters that approximate the phase of the baroclinic waves, such as sea level pressure and vertical velocity. *Tselioudis et al.* [2000] found that differences in shortwave fluxes between low and high pressure regimes in the Northern midlatitudes range seasonally between −5 and −50 W/m^2, while differences in longwave fluxes range between 5 and 35 W/m^2. *Norris and Iacobellis* [2005] documented synoptic cloud variations associated with changes in vertically averaged temperature, stratification, mid-tropospheric vertical velocity, and SST advection and used the results to infer the response of midlatitude oceanic clouds to climate change. They found that a vertically uniform warming would result in decreased cloud amount and optical thickness over a large range of dynamical conditions, implying an overall positive feedback on the climate system. They also found that a decrease in the variance of vertical velocity would lead to a small decrease in mean cloud optical thickness and top height, implying a positive (negative) feedback in the event of a decrease (increase) in the strength of the midlatitude storm track.

[3] The large radiative differences between midlatitude dynamic regimes indicate that midlatitude climate feedbacks can result both from changes with climate in the frequency and the intensity of those regimes. In climate warming scenarios, the potential for systematic changes in the strength of the midlatitude circulation is present, both because of possible decreases in the meridional temperature gradient and the land-ocean temperature contrasts and of thermodynamical issues related to increases in the moisture availability in the troposphere. The overall evidence from the analysis of midlatitude data over the past 100 years points toward decreases in overall storm frequency but increases in average storm intensity [e.g., *Fyfe*, 2003]. Indirect evidence of changes in midlatitude storm properties were inferred from analyses of historical precipitation data for the continental US, which found significant increases in extreme precipitation events in the past 70 to 90 years [e.g., *Karl and Knight*, 1998]. Climate model studies of increased CO2 climate conditions indicate that the signature of fewer but more intense midlatitude storm events that has been found in the analyses of historical data can also be found in climate warming model simulations [*Carnell and Senior*, 1998; *Tselioudis et al.*, 2000; *Geng and Sugi*, 2003]. *Carnell and Senior* [1988] analyzed several climate-warming runs with the UKMO climate model and found decreases in the number of storms caused by decreases in shallow and medium strength storms but increases in the deep storm category. The potential for systematic midlatitude storm changes with climate warming, combined with the coupling between midlatitude atmospheric dynamics and radiation and precipitation, suggests the need to understand and quantify changes in midlatitude radiation and precipitation with storm strength and frequency.

[4] The objectives of the present study are twofold. First, we use current climate observations to quantify the relationships between midlatitude storm strength and frequency and radiation and precipitation. To do this we construct statistical composites of radiation and precipitation over storm domains similar to those derived by *Lau and Crane* [1995] and quantify changes in radiation and precipitation with storm strength. We do not consider the effect of possible latitudinal shifts of the storms or of direct temperature effects on cloud/precipitation properties. Second, we use the midlatitude

0094-8276/06/2005GL024513$05.00

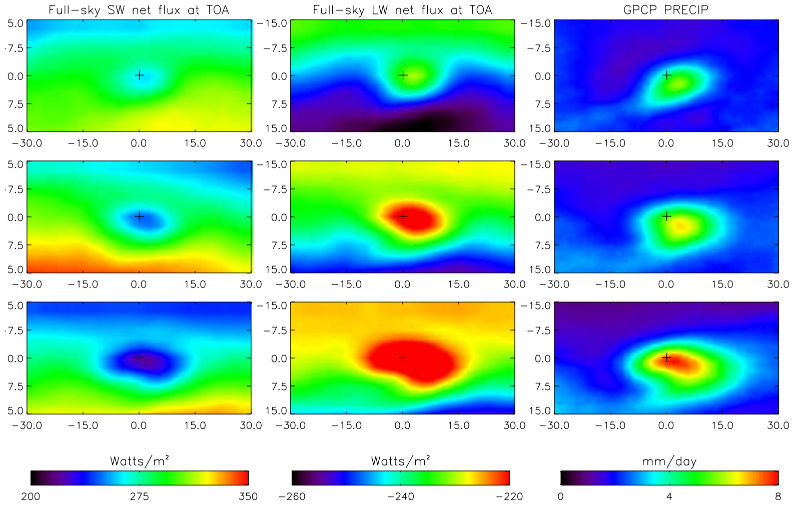

Figure 1. Top-of-the-atmosphere (TOA) net shortwave (left column) and net longwave flux (middle column), and precipitation (right column) for weak (top row), medium (middle row), and strong (bottom row) storms during NH summer.

storm changes with climate-warming predicted by the UKMO climate model [*Carnell and Senior*, 1998] and the observed radiation/precipitation-storm relationships to determine the radiation and precipitation changes to an increase in midlatitude storm intensity and a decrease in midlatitude storm frequency. This analysis is only a hypothetical scenario because we lack direct observations of how the storms will change in a warming climate. The analysis presented in this part illustrates a methodology for the use of current real climate relationships to make quantitative predictions of future climate radiation and precipitation changes.

2. Methodology

[5] To characterize the relationships between clouds, radiation, precipitation and dynamic conditions in midlatitude (30°–65° N/S) cyclonic storms, we composite observations of these quantities in the region surrounding each storm center for the period from March 1997 to September 2001. A storm tracking algorithm is applied to 6-hourly sea level pressure (SLP) data from the NCEP reanalysis [*Kalnay et al.*, 1996] to identify closed low pressure centers and to track them through their lifecycle. This version of the tracking algorithm identifies local minima in the SLP anomaly field (SLPA, the anomaly with respect to the local monthly SLP) rather than the SLP value itself. SLP-based storm tracking produce storm tracks that in the Northern Hemisphere (NH) concentrate almost exclusively over oceanic regions and in the Southern Hemisphere (SH) increase monotonically in intensity as one moves poleward. Use of SLPA produces more tracks over NH continental regions and reduces (but does not eliminate) the storm strength gradient in the southern hemisphere.

[6] Each storm is classified by its maximum strength (minimum SLPA) as weak, middle and strong. The SLPA ranges that define these strength categories are derived by dividing the frequency distribution of SLPA for the 5-year period into three equally populated parts. Once all storm centers are identified, observations of cloud, radiation, precipitation, and meteorological properties located in a 30-degree-latitude by 60-degree-longitude box centered on each storm center (at 2.5 degree intervals) are collected and averaged, separately for each season and for northern and southern zones, over the entire time period to produce composite maps for storms in each strength category. Observations included in the compositing step are cloud properties from the International Satellite Cloud Climatology Project D1 data set (ISCCP [*Rossow and Schiffer*, 1999]), radiative fluxes and atmospheric heating from the ISCCP-Flux Data [*Zhang et al.*, 2004], precipitation from the Global Precipitation Climatology Project [*Adler et al.*, 2003] and basic meteorology (winds, temperature and humidity) from the NCEP/NCAR reanalysis. This study will present only composites of radiation and precipitation fields but will describe the cloud property distributions that produce those composites.

[7] The storm composites provide a comprehensive look at the complex relationships between radiation, precipitation and the strength of midlatitude storms. In addition, the radiation and precipitation distributions of all regions that do not fall within a storm box are collected and composited for the whole region. This allows for contrasting the radiation and precipitation changes between storm and non-storm conditions.

3. Radiation/Precipitation Composites

[8] Figure 1 shows composites of top-of-the-atmosphere (TOA) net shortwave (or absorbed shortwave) radiation, TOA net longwave radiation, and precipitation for all storm categories in Northern Hemisphere summer (selected for the larger shortwave fluxes). Note that TOA net longwave flux is plotted as minus the outgoing longwave radiation (OLR). Composites are centered on the SLPA minimum and show the radiation, and precipitation structures that we expect to see in the vicinity of midlatitude storms and that have been observed in other analyses of satellite and surface data [*Lau and Crane*, 1995]. Thick high clouds are concentrated in the northeast quadrant of the low-pressure center and along the frontal zones and produce minima in net

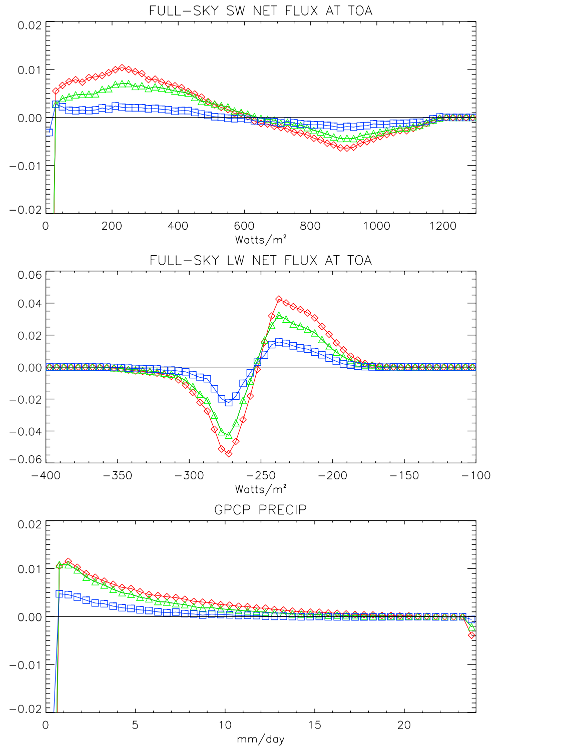

Figure 2. Probability Distribution Function differences between strong (red line), medium (green line), and weak (blue line) storms with respect to non-storm values for TOA net shortwave flux (top), TOA net longwave flux (middle), and precipitation (bottom).

shortwave flux and OLR along with maxima in precipitation. Lower, thinner clouds in the vicinity of the high-pressure centers trailing the fronts produce maxima in net shortwave flux and OLR and negligible amounts of precipitation.

[9] The novelty of the present results is that they illustrate and quantify the changes in cloud, radiation, and precipitation with the strength of the midlatitude storm systems. To first order, the increase in storm strength increases both the reflectivity and height of the clouds near the storm center, as well as the areal coverage of the storm box by high, thick clouds with large precipitation amounts. Net TOA shortwave radiation shows minima of about 218 W/m^2 (peak reflectivity) in strong storms that increase to about 254 W/m^2 in weak storms. OLR minima are about 209 W/m^2 in strong storms and about 240 W/m^2 in weak storms. Peak precipitation amounts reach 8 mm/day in strong storms and only 6 mm/day in weak storms.

[10] The differences in these quantities between storm and non-storm regimes are also examined. One can think of the non-storm regime as the anti-cyclonic portion of the baroclinic wave characterized by generally weaker motions. The results are illustrated in Figure 2, where the differences in frequency distributions between strong, medium, and weak storms with respect to non-storm values are presented, for TOA net shortwave flux, TOA net longwave flux, and precipitation. The histograms are derived from all 2.5 degree grid cells that belong to storm boxes of the three categories and to non-storm events. The shortwave and longwave distribution differences show that storm regimes are shifted toward higher reflection and lower emittance values than the non-storm field, increasing so as storm strength increases. Weak storms show only small radiation differences from the non-storm field, particularly in the shortwave flux distributions. Note that the shortwave flux distributions include zero values that correspond to nighttime. In the precipitation distributions, all storm categories show higher frequencies of all precipitation values than the non-storm field and lower frequencies of zero precipitation occurrences. Strong and medium strength storms show the largest differences from the non-storm precipitation values while weak storm events show much smaller differences from the non-storm events.

4. Implied Climate Effects

[11] The storm composites in the previous section show how radiation and precipitation fields change with the strength of midlatitude storms. Observational and modeling studies indicate that a warmer climate may contain fewer but stronger midlatitude storms. The UKMO model simulations of *Carnell and Senior* [1998] show that, in a doubled-CO2 climate, average Northern midlatitude storm frequency will decrease by about 7%, due to decreases by 7% and 5% in weak and medium strength storms, respectively, and increases by 5% in strong storms. The radiation and precipitation composites of the previous section are used to estimate the changes in the radiation and precipitation fields that would be produced by such storm strength and frequency changes. To keep this hypothetical scenario simple, the Northern midlatitude winter storm changes of the UKMO model are applied to storm composites in both hemispheres and for both seasons. This allows us to isolate hemispheric and seasonal differences of the radiation/precipitation storm responses that are only due to the different observed relationships between storm strength and radiation/precipitation. The calculation is performed in two stages. In the first stage the relative changes in storm strength are applied to the storm composites to calculate the effect of the shift in storm strength distribution on the radiation and precipitation fields. In the second stage the changes in storm frequency are applied to both the storm and non-storm composites to calculate the effect of the decrease in storm frequency on the radiation and precipitation fields.

[12] The results for the TOA net shortwave and longwave radiation are shown in Table 1 for the summer and winter seasons in the two hemispheres. For the shortwave flux, the increase in storm strength produces a cooling effect due to the increase in the average reflectivity of the storm clouds. This effect varies between 1.9 and 4.9 W/m^2 and is stronger in the southern hemisphere where the background albedo is lower. The decrease in storm frequency produces a shortwave warming due to the decrease in total cloud cover. This effect varies between 1.4 and 2.6 W/m^2. As a result, the combined shortwave effect of the storm changes is almost everywhere a cooling that varies from 0 to 3.5 W/m^2. For the longwave flux, the increase in storm strength produces a warming effect due to the increase in the average height of the storm clouds. The warming varies from 1.4 to 2.5 W/m^2. The decrease in storm frequency produces a longwave

Table 1. Net TOA Shortwave and Longwave Flux Changes With Storm Strength and Frequency

	30°N–65°N DJF		30°N–65°N JJA	
	SW, W/m^2	LW, W/m^2	SW, W/m^2	LW, W/m^2
Storm strength ↑	−3,7	+1.5	−1.9	+1.6
Storm frequency↓	+2.6	−1.4	+1.9	−1.0
Total	−1.1	+0.1	0.0	+0.6
	30°N–65°S JJA		30°N–65°S DJF	
	SW, W/m^2	LW, W/m^2	SW, W/m^2	LW, W/m^2
Storm strength↑	−4.9	+2.5	−3.7	+1.4
Storm frequency↓	+1.4	−0.3	+1.9	−0.4
Total	−3.5	+2.2	−1.8	+1.0

cooling due to the decrease in cloud cover. This effect varies between 0.3 and 1.4 W/m^2. As a result, the net longwave effect of the two storm changes is a warming effect that varies between 0.1 and 2.2 W/m^2.

[13] The results for the precipitation field are summarized in Table 2 for the winter and summer of the northern hemisphere. Southern hemisphere precipitation composites were not used in this calculation because the GPCP precipitation retrievals exhibit very strong precipitation decreases with latitude in the southern midlatitudes that may be an underestimate because of the inability of the microwave retrievals to sense ice precipitation. The increase in storm strength produces precipitation increases of 0.08–0.1 mm/day and the decrease in storm frequency produces precipitation decreases of 0.02–0.03 mm/day. The net storm effect is dominated by the increase in storm strength, an increase of 0.05–0.08 mm/day.

5. Discussion

[14] The storm composites presented here show large changes in radiation and precipitation with storm strength. When those changes are assumed to apply in a model-based scenario of global warming-induced storm changes, they produce shortwave cooling of 0–3.5 W/m^2 and longwave warming of 0.1–2.2 W/m^2. These effects are significant since they translate into global effects of about 1 W/m^2 on average (assuming no other changes) while cloud feedbacks in climate models vary between 0 and 3 W/m^2 [*Colman*, 2003]. In both the shortwave and longwave results, the increase in storm strength dominates the decrease in storm frequency, producing higher and thicker clouds that result in the shortwave cooling and longwave warming effects. This result is in agreement with the analysis of *Norris and Iacobellis* [2005] that finds increases in cloud optical depth and top height in the event of intensification of the northern midlatitude storms.

[15] For precipitation the increase in strong storms also dominates the decrease in storm frequency and produces an increase in precipitation of 0.05–0.08 mm/day. Given that the average precipitation in the northern midlatitudes is around 2 mm/day, this change amounts to a 3–4% increase in precipitation. The change is relatively small due to the fact that average precipitation does not vary too much between the three storm categories and the non-storm events. This in turn may be due to the selection of large box sizes for the storm extractions that were meant to cover the area of influence of the storm on the cloud and radiation fields.

Table 2. Net Precipitation Changes With Storm Strength and Frequency

	Precipitation 30°N–65°N, mm/day	
	DJF	JJA
Storm strength↑	+0.10	+0.08
Storm frequency↓	−0.02	−0.03
Total	+0.08	+0.05

[16] This study shows well-defined relationships between midlatitude storm dynamics and the resulting radiation and precipitation. It is important to evaluate the ability of climate models to simulate both the qualitative and quantitative characteristics of these relationships to test the models' ability to simulate dynamics-induced midlatitude cloud feedbacks. In addition, this study presents a methodology that utilizes current climate relationships and climate change model predictions to derive quantitative and more complete estimates of radiation and precipitation changes that might accompany climate changes. Given the recent large increases in the amount and quality of climate observations, such studies can be used in tandem with model simulations to derive climate change estimates for parameters and processes that are heavily parameterized in climate model codes.

[17] **Acknowledgments.** The authors wish to thank Allyson Polak for technical assistance with the data analysis. Funding for this study comes from the NASA MAP (D. Anderson) and DOE ARM (W. Ferrell) programs.

References

Adler, R. F., et al. (2003), The version 2 Global Precipitation Climatology Project (GPCP) monthly precipitation analysis (1979-present), *J. Hydrometeorol.*, *4*, 1147–1167.

Carnell, R. E., and C. A. Senior (1998), Changes in mid-latitude variability due to increasing greenhouse gasses and sulphate aerosols, *Clim. Dyn.*, *14*, 369–383.

Colman, R. (2003), A comparison of climate feedbacks in general circulation models, *Clim. Dyn.*, *20*, 865–873.

Fyfe, J. C. (2003), Extratropical southern hemisphere cyclones: Harbingers of climate change?, *J. Clim.*, *16*, 2802–2805.

Geng, Q., and M. Sugi (2003), Possible change of extratropical cyclone activity due to enhanced greenhouse gases and sulfate aerosols—Study with a high resolution AGCM, *J. Clim.*, *16*, 2262–2274.

Kalnay, E., et al. (1996), The NMC/NCAR 40-Year Reanalysis Project, *Bull. Am. Meteorol. Soc.*, *77*, 437–471.

Karl, T. R., and R. W. Knight (1998), Secular trends in precipitation amount, frequency, and intensity in the United States, *Bull. Am. Meteorol. Soc.*, *79*, 231–261.

Lau, N.-C., and M. W. Crane (1995), A satellite view of the synoptic scale organization of cloud properties in midlatitude and tropical circulation systems, *Mon. Weather Rev.*, *123*, 1984–2006.

Norris, J. R., and S. F. Iacobellis (2005), North Pacific cloud feedbacks inferred from synoptic-scale dynamic and thermodynamic relationships, *J. Clim.*, in press.

Rossow, W. B., and R. A. Schiffer (1999), Advances in understanding clouds from ISCCP, *Bull. Am. Meteorol. Soc.*, *80*, 2261–2288.

Tselioudis, G., Y.-C. Zhang, and W. B. Rossow (2000), Cloud and radiation variations associated with northern midlatitude low and high sea level pressure regimes, *J. Clim.*, *13*, 312–327.

Zhang, Y.-C., W. B. Rossow, A. A. Lacis, V. Oinas, and M. I. Mishchenko (2004), Calculation of radiative fluxes from the surface to top of atmosphere based on ISCCP and other global data sets: Refinements of the radiative transfer model and the input data, *J. Geophys. Res.*, *109*, D19105, doi:10.1029/2003JD004457.

W. B. Rossow, NASA Goddard Institute for Space Studies, Columbia University, 2880 Broadway, New York, NY 10025, USA.

G. Tselioudis, Department of Applied Physics and Applied Mathematics, Columbia University, 2880 Broadway, New York, NY 10025, USA. (gtselioudis@giss.nasa.gov)